

**John Carroll University**

---

From the Selected Works of Jeffrey Dyck

---

December 15, 2003

# Magnetic and transport properties of the V<sub>2</sub>–VI<sub>3</sub> diluted magnetic semiconductor Sb<sub>2</sub>–<sub>x</sub>Mn<sub>x</sub>Te<sub>3</sub>

Jeffrey S. Dyck, *John Carroll University*

P. Svanda

P. Lostak

J. Horak

W. Chen, *University of Michigan - Ann Arbor*, et al.



Available at: [https://works.bepress.com/jeffrey\\_dyck/9/](https://works.bepress.com/jeffrey_dyck/9/)

# Magnetic and transport properties of the $V_2-VI_3$ diluted magnetic semiconductor $Sb_{2-x}Mn_xTe_3$

J. S. Dyck<sup>a)</sup>

*Department of Physics, University of Michigan, Ann Arbor, Michigan 48109-1120*

P. Švanda and P. Lošťák

*Faculty of Chemical Technology, University of Pardubice, Čs. Legií Square 565, 532 10 Pardubice, Czech Republic*

J. Horák

*Joint Laboratory of Solid State Chemistry, Czech Academy of Sciences and University of Pardubice, Studentská 64, 530 09 Pardubice, Czech Republic*

W. Chen and C. Uher

*Department of Physics, University of Michigan, Ann Arbor, Michigan 48109-1120*

(Received 10 July 2003; accepted 23 September 2003)

We have measured electrical and magnetic properties of single crystals of  $Sb_{2-x}Mn_xTe_3$  with  $x = 0-0.045$  at temperatures of 2 K to 300 K. Hall effect measurements indicate that each manganese atom donates approximately one hole to the valence band. The magnetic susceptibility is paramagnetic down to 2 K, and both Curie-Weiss and Brillouin analyses show that manganese substitutes for Sb and takes the  $Mn^{2+}$  state with  $S = 5/2$ . Contrary to the case of III-V host matrices, manganese does not stimulate ferromagnetic order in the family of bulk layered  $V_2-VI_3$  diluted magnetic semiconductors, at least in the range of magnetic impurity and carrier concentrations studied here. © 2003 American Institute of Physics. [DOI: 10.1063/1.1626803]

## I. INTRODUCTION

There has been a great deal of recent research activity on the incorporation of magnetic ions into semiconductors to produce ferromagnetism. Most of the past attention has been focused on the (Ga,Mn)As (Ref. 1) and (In,Mn)As (Ref. 2) systems. Recently, we have acquired an understanding of the importance of defects in as-grown and annealed layers,<sup>3,4</sup> and in increasing the Curie temperature  $T_C$  in (Ga,Mn)As from  $\sim 110$  K to 150 K in ultrathin films.<sup>5</sup> Unfortunately, it is not clear whether this system will have a fundamental upper limit to the Curie temperature.<sup>6,7</sup> Alternative candidate semiconductor hosts therefore should be investigated for their potential for room-temperature ferromagnetism. Also, research along these lines could enable a more detailed understanding of ferromagnetism in semiconductors, in general.

A number of other Mn-doped III-V-based semiconductors have been studied, such as (Ga,Mn)P,<sup>8</sup> (Ga,Mn)N,<sup>9</sup> and (Ga,Mn)Sb.<sup>10</sup> Additional systems have included GeMn,<sup>11,12</sup> transition metal-doped ZnO (Ref. 13) and  $TiO_2$ ,<sup>14</sup> and Mn-doped II-IV- $V_2$  chalcopyrite semiconductors.<sup>15</sup> The most popular magnetic ion sought to stimulate magnetic order in these compounds is clearly Mn, followed by Co. Notable exceptions are single crystal forms of  $Sb_{2-x}V_xTe_3$ , which display<sup>16</sup> Curie temperatures as high as 25 K for  $x = 0.03$ , and  $Bi_{2-x}Fe_xTe_3$ , which attains (Ref. 17)  $T_C = 12$  K for  $x_{Fe} = 0.08$ . Antimony telluride ( $Sb_2Te_3$ ) is a narrow-gap semiconductor ( $E_g \sim 0.26$  eV) that belongs to the group of tetradymite-type layered compounds having the formula

$A_2^yB_3^{VI}$  (with  $A = Sb, Bi$  and  $B = Se, Te$ ). Crystals in this family are composed of repeated planes of five atomic layer lamella separated by a van der Waals gap. In vanadium-doped  $Sb_2Te_3$ , this layered structure induces an unusually large magnetic anisotropy with the easy axis parallel to the  $c$  axis (perpendicular to the plane). Furthermore, their bulk nature affords the opportunity to study an equilibrium diluted magnetic semiconductor (DMS) structure using a wider array of techniques than are available for thin films. A logical extension to this discovery is to investigate the effect of Mn doping in this tetradymite-type host material.

There is a report on  $Sb_{2-x}Mn_xTe_3$  in the literature<sup>18</sup> for concentrations of manganese up to about  $x = 0.007$ . Paramagnetic resonance and magnetic susceptibility results suggested a magnetic moment of  $1.8 \mu_B$  per Mn atom. Reflectivity data indicated an increase in the hole concentration at the rate of approximately 1 hole per Mn atom. These facts led the authors to conclude that Mn substitutes for Sb and is in a low spin  $(t_{2g})^5(e_g)^0$  state where only one electron is unpaired. However, the measurements were limited to temperatures above 77 K. We were interested in exploring higher concentrations of Mn in  $Sb_2Te_3$  down to liquid-helium temperatures, and to look for the presence of magnetic order.

## II. EXPERIMENT

Single crystals of  $Sb_{2-x}Mn_xTe_3$  with nominal  $x$  values between 0 and 0.04 were grown using the Bridgman method. Polycrystalline starting material was synthesized by heating stoichiometric mixtures of 99.999% pure Sb, Te, and Mn to 1073 K for 48 h in sealed evacuated conical quartz am-

<sup>a)</sup>Present address: Department of Physics, John Carroll University, University Heights, OH 44118; electronic mail: jdyck@jcu.edu

TABLE I. Results of the Curie–Weiss fitting for single crystal  $\text{Sb}_{2-x}\text{Mn}_x\text{Te}_3$ . Also given are the concentration of manganese atoms as determined from EMPA ( $x$ ) and from fitting to a Brillouin function assuming  $S=5/2$  ( $x^*$ ). Effective Bohr magneton numbers calculated using the Mn content from EPMA ( $p_{\text{eff}}$ ) and from the Brillouin analysis ( $p_{\text{eff}}^*$ ) are included.

$x$ (from EMPA)	$C$ [ $\text{cm}^3 \text{g}^{-1} \text{K}^{-1}$ ]	$\theta_{CW}$ (K)	$\chi_0$ ( $\text{cm}^3/\text{g}$ )	$p_{\text{eff}}$ ( $\mu_B/\text{Mn}$ ) ( $g=2$ , using $x$ )	$x^*$ (from M vs B)	$p_{\text{eff}}^*$ ( $\mu_B/\text{Mn}$ ) ( $g=2$ , using $x^*$ )
$0.003 \pm 0.0008$	$1.8292 \times 10^{-5}$	0.3017	$-3.4895 \times 10^{-7}$	5.529	0.0027	5.828
$0.004 \pm 0.0007$	$2.2789 \times 10^{-5}$	0.3000	$-3.3785 \times 10^{-7}$	5.345	0.0034	5.797
$0.007 \pm 0.001$	$3.593 \times 10^{-5}$	0.3006	$-2.942 \times 10^{-7}$	5.073	0.0054	5.776
$0.030 \pm 0.002$	$1.993 \times 10^{-4}$	0.2649	$-1.955 \times 10^{-8}$	5.771	0.0295	5.820
$0.045 \pm 0.002$	$2.612 \times 10^{-4}$	0.2524	$9.567 \times 10^{-8}$	5.395	0.0380	5.871

poules. The ampoules were then annealed at 1000 K for 24 h in a vertical Bridgman furnace and lowered into a temperature gradient of 125 K/cm at a rate of 1.3 mm/h. Specimens for measurements were cut from the middle of the obtained single crystals with a spark erosion machine. Powder x-ray diffraction and electron microprobe analysis (EMPA) were employed to analyze the structure and stoichiometry. Actual compositions are presented in Table I.

Transport and magnetic property measurements were carried out on the *same samples* from temperatures of 2 K to 300 K. Magnetic susceptibility and magnetization measurements were made in a Quantum Design superconducting quantum interference device magnetometer equipped with a 5.5 T magnet. Hall effect and electrical resistivity data were collected in the same instrument with the aid of a Linear Research ac bridge with 16 Hz excitation.

### III. RESULTS

Figure 1 shows the powder x-ray data for the specimen with highest Mn content ( $x=0.045$ ). All observed lines indexed to the tetradymite crystal structure and no secondary phases were detected. Furthermore, EMPA results verified that the distribution of Mn atoms was uniform within the detection limits and that the composition was close to the nominal stoichiometry. The lattice parameters and  $c/a$  ratio

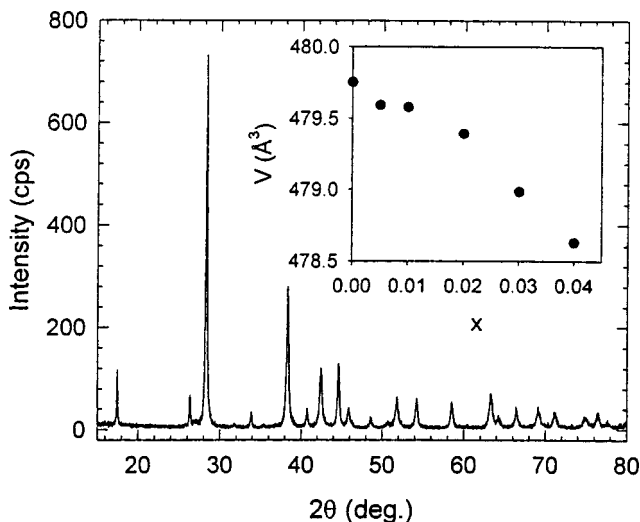


FIG. 1. X-ray powder diffraction data for  $\text{Sb}_{1.955}\text{Mn}_{0.045}\text{Te}_3$ . All peaks can be indexed to the tetradymite crystal structure, with no impurity phases detected. The inset displays the decreasing trend in the unit-cell volume with increasing manganese content.

were weakly dependent on  $x$ , though we note that the unit cell volume (shown in the inset to Fig. 1) has a decreasing trend with Mn content. This fact indicates that the majority of the manganese atoms are incorporated onto host lattice sites rather than interstitially.

In-plane electrical resistivity (current perpendicular to the  $c$  axis) of  $\text{Sb}_2\text{Te}_3$  is dominated by hole conduction and has a metallic temperature dependence characteristic of a degenerately doped semiconductor. The typical carrier concentration is  $p \sim 1 \times 10^{20} \text{cm}^{-3}$  due to the presence of a large number of native antisite defects.<sup>19</sup> As shown in Fig. 2, the addition of manganese leads to a reduction of the resistivity and a decrease of the Hall coefficient which is consistent with hole doping. At low  $x$ , these results agree with those of Horak *et al.*,<sup>18</sup> while for values of  $x > 0.01$ , the doping rate is somewhat less than 1 hole per Mn atom. One possible expla-

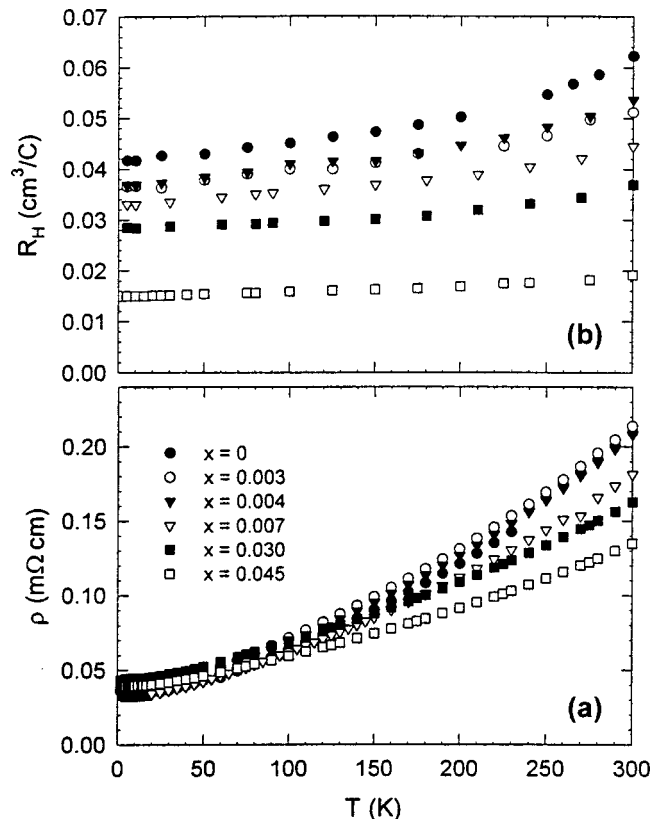


FIG. 2. (a) Electrical resistivity  $\rho$  and (b) Hall coefficient  $R_H$  data as a function of temperature for the series of  $\text{Sb}_{2-x}\text{Mn}_x\text{Te}_3$  single crystals. Current is perpendicular to the  $c$  axis, and magnetic field (for Hall) is parallel to the  $c$  axis.

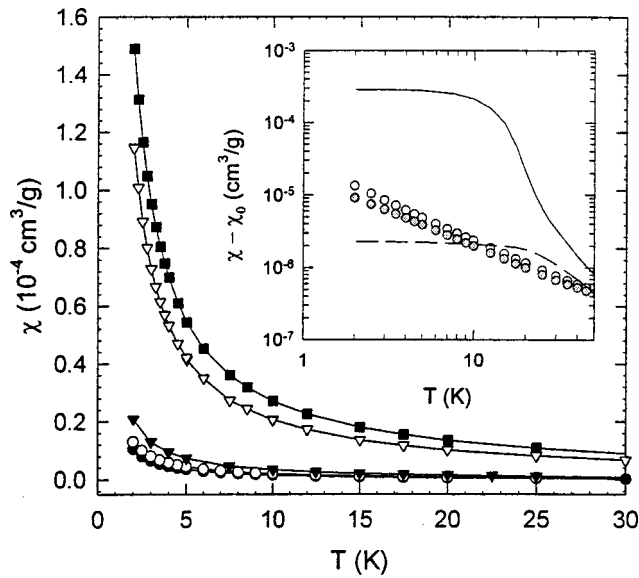


FIG. 3. Magnetic susceptibility  $\chi$  versus temperature for the series of  $\text{Sb}_{2-x}\text{Mn}_x\text{Te}_3$  single crystals. Symbol definitions are given in Fig. 2. The inset plots the magnetic susceptibility, corrected for the small diamagnetic contribution of the host lattice, versus temperature for  $\text{Sb}_{1.996}\text{Mn}_{0.004}\text{Te}_3$  (open circle for  $B\parallel c$  and gray circle for  $B\perp c$ ) and  $\text{Sb}_{1.97}\text{V}_{0.03}\text{Te}_3$  (solid line for  $B\parallel c$  and dashed line for  $B\perp c$ ).

nation for this is that the presence of Mn begins to affect the concentration of native defects,<sup>20–22</sup> hence altering the number of background carriers due to the latter. In contrast to the effect of vanadium on  $\text{Sb}_2\text{Te}_3$ , there is no anomaly in these transport properties at low temperatures associated with a transition to a magnetically ordered state.

Figure 3 displays the temperature dependence of the magnetic susceptibility for the  $\text{Sb}_{2-x}\text{Mn}_x\text{Te}_3$  single crystals with the applied magnetic field ( $B = 1000$  G) parallel to the  $c$  axis. Antimony telluride is diamagnetic<sup>23</sup> and we measure a temperature independent value of  $\chi = -3.8 \times 10^{-7} \text{ cm}^3/\text{g}$ . Samples containing Mn have a paramagnetic susceptibility. The data fit very nicely to a Curie–Weiss law of the form  $\chi(T) = C/T - \theta_{CW} + \chi_0$  where  $C$  is the Curie constant,  $\theta_{CW}$  is the paramagnetic Curie temperature, and  $\chi_0$  is the temperature independent diamagnetic contribution of the host  $\text{Sb}_2\text{Te}_3$  crystal. The fitting parameters are given in Table I. Calculations of the effective Bohr magneton number  $p_{\text{eff}}$  are made via the equation  $C = Np_{\text{eff}}^2\mu_B^2/3k_B$ , where  $N$  is the number of Mn ions (we take the EMPA value),  $\mu_B$  is the Bohr magneton number, and  $k_B$  is Boltzmann’s constant. Values of  $p_{\text{eff}} = g\sqrt{J(J+1)}$  are close to the value for high spin  $\text{Mn}^{2+}$  ( $L = 0, S = 5/2$ ) of  $5.92 \mu_B$  taking the Landé  $g$  factor to be  $g = 2$ . With  $\theta_{CW} \leq 0.3$  K, there is clearly no strong tendency toward ferromagnetic order among the spins. We also note that  $\chi_0$  values arising from the fitting analysis are very close to the expected value for  $\text{Sb}_2\text{Te}_3$  for small  $x$ , and become less negative as  $x$  increases. This trend is consistent with a small (positive) Pauli paramagnetic contribution associated with the increased concentration of holes arising from the Mn substitutional ions.

The inset to Fig. 3 displays the stark difference in the magnetic susceptibilities between Mn-doped and V-doped  $\text{Sb}_2\text{Te}_3$ . Spins in  $\text{Sb}_{2-x}\text{V}_x\text{Te}_3$  order magnetically when the

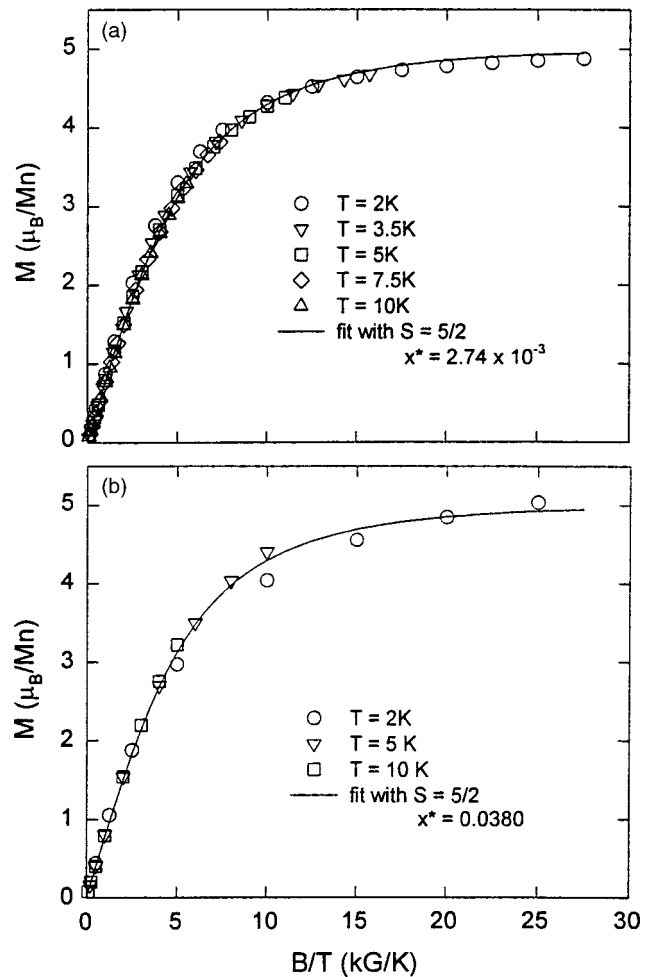


FIG. 4. Magnetization curves for single crystals of (a)  $\text{Sb}_{1.997}\text{Mn}_{0.003}\text{Te}_3$  and (b)  $\text{Sb}_{1.955}\text{Mn}_{0.045}\text{Te}_3$  at several temperatures. Magnetic field  $B$  is oriented parallel to the  $c$  axis. Solid lines are fits of the data to a Brillouin function assuming  $S = 5/2$  where the manganese content  $x^*$  is a fitting parameter.

magnetic field is parallel to the  $c$  axis; but for fields perpendicular to the  $c$  axis, the magnetization is more than two orders of magnitude smaller. In contrast, the anisotropy in  $\text{Sb}_{2-x}\text{Mn}_x\text{Te}_3$  is much smaller ( $B\parallel c$  orientation is  $\leq 50\%$  larger than  $B\perp c$  orientation) and  $\chi(T)$  remains paramagnetic down to 2 K for values of  $x$  up to 0.045. A discussion of this behavior is deferred to a later section of the article.

Low-temperature magnetization data add further experimental evidence for the high spin  $\text{Mn}^{2+}$  state in  $\text{Sb}_{2-x}\text{Mn}_x\text{Te}_3$ . The data at several temperatures below 10 K for each composition were fit with a single Brillouin function with spin  $S$  and concentration of  $\text{Mn } x^*$  as free parameters. For all samples,  $S = 5/2$  to within 5% and  $x^*$  was close to the content  $x$  determined from EMPA. Figure 4(a) shows  $M$  versus  $B/T$  at several temperatures between 2 K and 10 K for  $\text{Sb}_{1.997}\text{Mn}_{0.003}\text{Te}_3$ —the solid line is a fit to a Brillouin function with  $S = 5/2$  and where only  $x^*$  is a free parameter (see Table I). For the other compositions with  $x < 0.01$ , the analysis yields very similar results. For larger  $x$ , the data at  $T = 2$  K departs somewhat from the  $S = 5/2$  curve, though the fit does not improve with a different value of  $S$ . The  $M$  versus  $B$  curve for  $\text{Sb}_{1.955}\text{Mn}_{0.045}\text{Te}_3$  is shown in Fig. 4(b). Perhaps correlation among spins becomes important for these high

doping levels at temperatures near and below 2 K. Recalculated values of the effective Bohr magneton number  $p_{\text{eff}}^*$  using  $x^*$  rather than  $x$  are presented in Table I for comparison. For all samples,  $p_{\text{eff}}^*$  is even closer to the value of  $5.92 \mu_B$  per Mn expected for the  $S=5/2$  state than values of  $p_{\text{eff}}$  calculated from  $x$ .

#### IV. DISCUSSION

With strong evidence for the predominance of the  $\text{Mn}^{2+}$  state, we can postulate the location of the substitutional ions in the lattice. In pure  $\text{Sb}_2\text{Te}_3$ , each Sb atom ( $5s^25p^3$ ) supplies three electrons and each Te ( $5s^25p^4$ ) gains two in forming the  $\sigma$  bonds of the diamagnetic solid. Manganese ( $3d^54s^2$ ) apparently provides its two  $s$  electrons to bonding. Were it situated on Te sites, this atom would be deficient two electrons thereby creating two holes in the valence band, contrary to the Hall data indicating an approximate doping rate of one hole per Mn. Rather, a picture of Mn substituting for Sb, with the  $4s^2$  electrons of Mn replacing the  $5p^3$  electrons of Sb, would result in the observed doping rate of one hole per Mn. Our interpretation is consistent with Horak *et al.*,<sup>18</sup> though they calculate  $1.8 \mu_B$  per Mn from magnetic susceptibility data, which implies a  $S=1/2$  state. According to Horak *et al.*,<sup>18</sup> this low spin arrangement can be understood by considering that the  $d$  orbitals of the Mn atom will be split by the octahedral field of the six Te atoms into a triply degenerate lower  $t_{2g}$  orbital and a doubly degenerate  $e_g$  orbital. Provided the crystal-field splitting is large enough, the five  $d$  electrons will fill only the  $t_{2g}$  orbital with two pairs of spin-paired electrons and a single unpaired electron. In contrast, our data provide strong evidence for the high spin  $S=5/2$  ( $t_{2g})^3(e_g)^2$  configuration implying that the crystal field splitting is too small to realize the  $(t_{2g})^5(e_g)^0$  configuration. This discrepancy is not understood at this time. However, we note that  $\text{Mn}^{2+}$  is commonly observed to reside in the high spin state in DMS structures.<sup>24,25</sup> In particular, Mn has  $S=5/2$  in  $\text{Pb}_{1-x}\text{Mn}_x\text{Te}$ . (Ref. 26), an environment where the Mn is also octahedrally coordinated by six Te atoms.

The fact that  $\text{Sb}_{2-x}\text{Mn}_x\text{Te}_3$  is paramagnetic is quite interesting given that  $\text{Sb}_{1.97}\text{V}_{0.03}\text{Te}_3$  is ferromagnetic below 25 K. One might assume that Mn with  $S=5/2$  would have a higher  $T_C$  than V with  $S=1$  (see Ref. 16). Further, we note that unlike vanadium, manganese adds holes to the valence band of  $\text{Sb}_2\text{Te}_3$  resulting in higher carrier concentrations in Mn-doped material. In the Zener model description of ferromagnetism in tetrahedrally bonded diluted magnetic semiconductors,<sup>27</sup> the Curie temperature increases with hole concentration  $p$  and magnitude of the spin  $S$ . For the Ruderman–Kittel–(Kasuya)–Yosida interaction, the dependence of  $T_C$  on  $p$  can be more complicated, having a Friedel oscillation behavior. More study is needed to determine if the origin of the ferromagnetic order in the tetradymite-type  $\text{A}_2\text{B}_2\text{VI}$  structure is similar to that in III–V and II–VI DMS materials.

#### V. CONCLUSIONS

In conclusion, we find that single crystals of  $\text{Sb}_{2-x}\text{Mn}_x\text{Te}_3$  for  $x=0.003$ – $0.045$  are paramagnetic down to

2 K. Both low-temperature magnetization data and low-field magnetic susceptibility data up to room temperature indicate five unpaired spins per manganese atom. Together with Hall data that reveal an approximate doping rate of one hole per Mn atom, these results show that Mn takes the divalent,  $S=5/2$  ( $3d^5$ ) electronic configuration. This article illustrates the rich magnetic phenomena that an alternative DMS system, namely, a tetradymite-type layered compound, can provide to aid in a more general understanding of magnetism in semiconductors.

#### ACKNOWLEDGMENTS

The authors gratefully acknowledge the support of NSF International Grant No. 0201114 and of the Ministry of Education of the Czech Republic under the project KON-TAKATME 513.

- <sup>1</sup>H. Ohno, A. Shen, F. Matsukura, A. Oiwa, A. Endo, S. Katsumoto, and Y. Iye, *Appl. Phys. Lett.* **69**, 363 (1996).
- <sup>2</sup>H. Ohno, H. Munekeata, T. Penney, S. von Molnar, and L. Chang, *Phys. Rev. Lett.* **68**, 2664 (1992).
- <sup>3</sup>S. J. Potashnik, K. C. Ku, S. H. Chun, J. J. Berry, N. Samarth, and P. Schiffer, *Appl. Phys. Lett.* **79**, 1495 (2001).
- <sup>4</sup>T. Hayashi, Y. Hashimoto, S. Katsumoto, and Y. Iye, *Appl. Phys. Lett.* **78**, 1691 (2001).
- <sup>5</sup>K. C. Ku, S. J. Potashnik, R. F. Wang, S. H. Chun, P. Schiffer, N. Samarth, M. J. Seong, A. Mascarenhas, E. Johnston-Halperin, R. C. Myers, A. C. Gossard, and D. D. Awschalom, *Appl. Phys. Lett.* **82**, 2302 (2003).
- <sup>6</sup>K. M. Yu, W. Walukiewicz, T. Wojtowicz, I. Kuryliszyn, X. Liu, Y. Sasaki, and J. K. Furdyna, *Phys. Rev. B* **65**, 201303(R) (2002).
- <sup>7</sup>K. M. Yu, W. Walukiewicz, T. Wojtowicz, W. L. Kim, X. Liu, U. Bindley, M. Dobrowolska, and J. K. Furdyna, preprint cond-mat/0303217 (2003).
- <sup>8</sup>N. Theodoropoulou, A. F. Hebard, M. E. Overberg, C. R. Abernathy, S. J. Pearton, S. N. G. Chum, and R. G. Wilson, *Phys. Rev. Lett.* **89**, 107203 (2002).
- <sup>9</sup>M. L. Reed, N. A. El-Masry, H. H. Stadelmaier, M. K. Rittums, M. J. Reed, C. A. Parker, J. C. Roberts, and S. M. Bedair, *Appl. Phys. Lett.* **79**, 3473 (2001).
- <sup>10</sup>X. Chen, M. Na, M. Cheon, S. Wang, H. Luo, B. D. McCombe, X. Liu, Y. Sasaki, T. Wojtowicz, J. K. Furdyna, S. J. Potashnik, and P. Schiffer, *Appl. Phys. Lett.* **81**, 511 (2002).
- <sup>11</sup>Y. D. Park, A. T. Hanbicki, S. C. Irwin, C. S. Hellberg, J. M. Sullivan, J. E. Mattson, T. F. Ambrose, A. Wilson, G. Spanos, and B. T. Jonker, *Science* **295**, 651 (2002).
- <sup>12</sup>S. Cho, S. Choi, S. C. Hong, Y. Kim, J. B. Ketterson, and J.-H. Jung, *Phys. Rev. B* **66**, 033303 (2002).
- <sup>13</sup>K. Ueda, H. Tabata, and T. Kawai, *Appl. Phys. Lett.* **79**, 988 (2001).
- <sup>14</sup>Y. Matsumoto, M. Murakami, T. Shono, T. Hasegawa, T. Fukumura, M. Kawasaki, P. Ahmet, T. Chikyow, S. Koshihara, and H. Koinuma, *Science* **291**, 854 (2001).
- <sup>15</sup>G. A. Medvedkin, T. Ishibashi, T. Nishi, K. Hayata, Y. Hasegawa, and K. Sato, *Jpn. J. Appl. Phys., Part 2* **39**, L949 (2000).
- <sup>16</sup>J. S. Dyck, P. Hajek, P. Lostak, and C. Uher, *Phys. Rev. B* **65**, 115212 (2002).
- <sup>17</sup>V. A. Kulbachinskii, A. Y. Kaminskii, K. Kindo, Y. Narumi, K. Suga, P. Lostak, and P. Svanda, *Physica B* **311**, 292 (2002).
- <sup>18</sup>J. Horak, M. Matyas, and L. Tichy, *Phys. Status Solidi A* **27**, 621 (1975).
- <sup>19</sup>G. R. Miller and C.-Y. Li, *J. Phys. Chem. Solids* **26**, 173 (1965); J. Horak, C. Drasar, R. Vovotny, S. Karamazov, and P. Lostak, *Phys. Status Solidi A* **149**, 549 (1995).
- <sup>20</sup>Z. Sary, L. Benes, and J. Horak, *Phys. Status Solidi A* **109**, 93 (1988).
- <sup>21</sup>T. Plechacek and J. Horak, *J. Solid State Chem.* **145**, 297 (1999).
- <sup>22</sup>P. Lostak, C. Drasar, A. Krejcova, L. Benes, J. S. Dyck, W. Chen, and C. Uher, *J. Cryst. Growth* **222**, 565 (2001).
- <sup>23</sup>A. Van Itterbeek, N. Van Deynse, and C. Herinckx, *Physica (Amsterdam)* **32**, 2123 (1966).

<sup>24</sup>*Diluted Magnetic Semiconductors*, Semiconductors and Semimetals Vol. 25, edited by J. K. Furdyna and J. Kossut (Academic Press, New York, 1988).

<sup>25</sup>H. Ohno, *J. Magn. Magn. Mater.* **200**, 110 (1999).

<sup>26</sup>M. Escorne, A. Mauger, J. L. Tholence, and R. Triboulet, *Phys. Rev. B* **29**, 6306 (1984).

<sup>27</sup>T. Dietl, H. Ohno, F. Matsukura, J. Cibert, and D. Ferrand, *Science* **287**, 1019 (2000).

Journal of Applied Physics is copyrighted by the American Institute of Physics (AIP). Redistribution of journal material is subject to the AIP online journal license and/or AIP copyright. For more information, see <http://ojps.aip.org/japo/japcr/jsp>  
Copyright of Journal of Applied Physics is the property of American Institute of Physics and its content may not be copied or emailed to multiple sites or posted to a listserv without the copyright holder's express written permission. However, users may print, download, or email articles for individual use.